Performance Evaluation of Multicarrier Systems Applied to Underwater Acoustic Communications

Iandra G. Andrade and Marcello L. R. de Campos

***Abstract*— In underwater acoustic communications, orthogonal frequency-division multiplexing (OFDM) is an alternative to frequency-shift keying (FSK). The key advantage of OFDM scheme is that it provides a significant increase in transmission rate. In this paper, we simulate and compare the performance in terms of bit-error rate (BER) of the OFDM and FSK in underwater acoustic communications. As an alternative we also analyze the behavior of single-carrier frequency-division multiplexing (SC-FDM). Lastly, to isolate the consequences of Doppler effect without masking distortions introduced by multi-path and the associated equalization procedures, their performances are also evaluated in the presence of Doppler and additive noise.**

***Keywords*— Underwater communication, OFDM, FSK, SC-FDM, Doppler.**

I. Introduction

In recent years there has been an increasing interest in underwater communications, essentially in its applications in military, scientific and civilian fields, including underwater security surveillance, communications to submarines, marine research, oceanography, marine commercial operation, the offshore industry, and exploration by autonomous underwater vehicles (AUV's).

A limiting factor of underwater communication is the complexity of the anisotropic medium. Variability of characteristics such as salinity, temperature and pressure makes the propagation velocity of acoustic waves change. These variations, together with transmitter and receiver relative motion, may also induce changes on transmitted signal, which are known as Doppler effect.

In order to benefit from the relative long range of propagation offered by acoustic waves, one must cope with possibly severe Doppler effect in a time-varying and frequency-selective channel.

Due to the physics of the medium, the useful bandwidth of the acoustic channel is a few tens of kHz, which makes high data rates challenging [1]. The desire for high data rate transmission in underwater communication, despite obstacles, is one of the motivations of this study.

A possible approach to achieve good spectral efficiency in underwater acoustic communication is to use a multicarrier modulation scheme. OFDM is a multicarrier system in which each subcarrier is chosen to be orthogonal to the others. However, drawbacks of OFDM are the high peak-to-average power ratio (PAPR) and possible hight sensitivity to subcarrier frequency drift.

A good candidate for the underwater acoustic communication in relatively high data rate is SC-FDM. One prominent advantage over OFDM is that the SC-FDM signal has lower PAPR and this characteristic brings benefits to mobile communications in terms of transmit power efficiency.

In this paper we present some relevant analysis and simulation results of FSK, OFDM and SC-FDM systems for narrowband underwater acoustic communications. Practical issues such as channel effects, Doppler and multipath are addressed. The paper is organized as follows. Section II briefly shows the channel model employed. In Section III FSK is presented. OFDM and SC-FDM techniques are exposed in Section IV as well as the PAPR problem of the OFDM system. The analyses of the simulation results are provided in Section V. Finally, conclusions are drawn in Section VI.

II. Underwater Acoustic Channel Modeling

Underwater acoustic channel supports time varying multiple propagation paths and each path has its time-dependent delay. Its specific characteristics is sparse echoes with long delay spreads brought by multiple reflections on sea bottom and surface [2]. The relative motion between transmitter and receiver as well as dynamics of the oceans cause Doppler effect on the received signal. When this effect is not negligible, it causes the transmitted signal to be dilated or compressed in time and its frequency band to be shifted, known as Carrier Frequency Offset (CFO) [3]. In this work Doppler effect was considered, but constant for all paths.

The channel impulse response model can be represented by [4]–[7]:

$$h\left(t\right)=\sum_{p=1}^{N_p}A_p\delta\left(t-\tau_p\left(t\right)\right), \tag{1}$$

where A_p is the path gain and $\tau_p\left(t\right)$ is the time varying delay associated with the pth path.

$$\tau_p\left(t\right)=\tau_p-a_pt, \tag{2}$$

τ_p is the path delay and a_p is the Doppler scaling factor defined as the ratio among the relative velocity and the velocity of the medium [5], [8]:

$$a_p=\frac{v_t-v_r}{c}. \tag{3}$$

Iandra G. Andrade and Marcello L. R. de Campos¸ Electrical Engineering Program, Federal University of Rio de Janeiro (UFRJ) Rio de Janeiro, Brazil, E-mails: iandra.galdino@smt.ufrj.br, campos@smt.ufrj.br. This work was partially supported by CNPq, CAPES (Prodefesa, 23038.009094/2013-83), FINEP (Comunicações Submarinas FINEP-01.13.0421.00), the Brazilian Navy Secretariat of CT&I/SECCTM, and the Institute of Sea Studies Admiral Paulo Moreira/IEAPM.

The path delay τ_p was assumed to be constant throughout the transmission. Furthermore, Doppler scaling factor was the same for all paths, hence we can represent a_p as a. Supposing that the major Doppler effect is caused by the transmitting and receiving motion, these assumptions are acceptable [9].

III. FSK System for Underwater Acoustic Communications

FSK is a digital modulation that maps information through discrete changes on carrier frequency. Each different symbol is mapped in a different carrier, therefore, the number of transmitted symbols is directly proportional to the number of available carriers. Lastly, the transmitter inserts a zero sequence at the beginning of each block to make a guard time (T_g) and prevent interference between successive transmitted blocks.

At the receiver side, the guard time is removed, a DFT is performed in each received symbol and so the energy of this symbol is calculated in order to estimate the transmitted symbol. Other noncoherent detection schemes can be used.

Figure 1 illustrates a typical, and much simple FSK system diagram. In FSK, carriers may be more spaced than in OFDM, which may render increased robustness to Doppler effect.

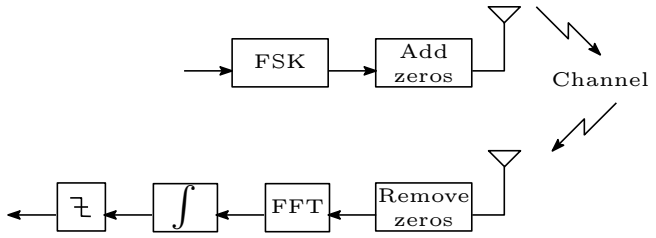

Fig. 1. Block diagram of an FSK system.

IV. OFDM and SC-FDM for Underwater Acoustic Communications

In this section, both transmitter and receiver structures of the SC-FDM and OFDM are compared in underwater acoustic scenario.

A. OFDM

The simplified block diagram of a typical OFDM system [10] is shown in Figure 2. In underwater, the OFDM signal is usually narrowband because of the low carrier frequency. The math model developed was based on this diagram.

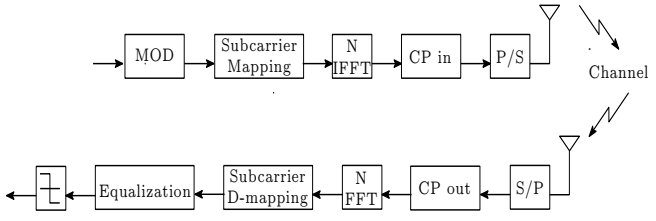

Fig. 2. Block diagram of an OFDM system.

The transmitter of an OFDM system first performs a digital modulation (MOD), in this case quadrature amplitude modulation (QAM), and than it groups the modulation symbols into K blocks containing N symbols, i.e., $\boldsymbol{s}[k] = [s_1(k), s_2(k) \ldots, s_N(k)]^T$. The processing is performed in parallel and all K symbol blocks are grouped into a matrix $\boldsymbol{S}[k], N \times K$. According to resource allocation, $\boldsymbol{S}[k]$ is mapped into N of M available orthogonal sub-carriers. This process is performed by the allocation matrix $\boldsymbol{D}$ defined by:

$$\boldsymbol{D} = \begin{bmatrix} \mathbf{0}_{(\frac{N-M}{2} \times M)} \\ \boldsymbol{I}_M \\ \mathbf{0}_{(\frac{N-M}{2} \times M)} \end{bmatrix} \in \mathbb{R}^{N \times M}, \tag{4}$$

resulting in $\boldsymbol{S}_d[k] = \boldsymbol{D}\boldsymbol{S}[k]$.

When all sub-carriers are used, $\boldsymbol{D}$ can be implemented as the identity matrix $\boldsymbol{I}_N$ and ($N = M$). After the sub-carrier mapping, the mapped frequency domain sequence is transformed back into complex time domain via an N-point inverse discrete Fourier transform (IDFT) denoted by ($\boldsymbol{F}_N^{-1}$), resulting in a signal which can be written as follows:

$$\boldsymbol{X}[n] = \boldsymbol{F}_N^{-1}\boldsymbol{S}_d[k], \quad \in \mathbb{C}^{N \times K}. \tag{5}$$

The last operation performed by the transmitter prior to transmission is to insert a set of L symbols, referring to the cyclic prefix (CP) whose length is L, assumed to be equal to or greater than the channel impulse response length ($L \geq L_c$), in order to provide a guard time and prevent inter-block interference (IBI) due to multi-path propagation. The signal after CP insertion can be expressed as:

$$\tilde{\boldsymbol{X}}[n] = \boldsymbol{T}_{CP}\boldsymbol{X}[n], \tag{6}$$

where $\boldsymbol{T}_{CP}$ is an $(N + L) \times N$ matrix, which adds a CP of length L. At the receiver side signal propagating through the channel can be modeled as a convolution between the channel impulse response and the transmitted data block. If CP is a copy of the last symbols of each block, the discrete time linear convolution can be converted into a discrete time circular convolution.

Assuming the channel impulse response as described in [6], i.e., $\boldsymbol{h}[n] = [h_1(n), h_2(n), \ldots, h_L(n)]^T$ is a multi-path channel time invariant during transmission, the received signal is the sum of echoes caused by the reflections of the transmitted signal on the sea surface and bottom [11] and can be expressed as follows:

$$\tilde{\boldsymbol{Y}}[n] = \boldsymbol{H}[n]\tilde{\boldsymbol{X}}[n] + \boldsymbol{V}[n], \tag{7}$$

where $\boldsymbol{H}[n]$ is the convolution matrix of the channel and $\boldsymbol{V}[n]$ is the additive white Gaussian noise (AWGN).

At the receiver side, the CP is removed by an $N \times (N + L)$ matrix $\boldsymbol{R}_{CP}$. This way, the received signal can be treated as a circular convolution between the transmitted signal and channel impulse response.

$$\boldsymbol{Y}[n] = \boldsymbol{R}_{CP}\boldsymbol{H}[n]\tilde{\boldsymbol{X}}[n] + \boldsymbol{R}_{CP}\boldsymbol{V}[n]. \tag{8}$$

From Equation (6) we have:

$$\begin{aligned} \boldsymbol{Y}[n] &= \boldsymbol{R}_{CP}\boldsymbol{H}[n]\boldsymbol{T}_{CP}\boldsymbol{X}[n] + \boldsymbol{R}_{CP}\boldsymbol{V}[n] \\ &= \boldsymbol{C}\boldsymbol{X}[n] + \boldsymbol{R}_{CP}\boldsymbol{V}[n], \end{aligned} \tag{9}$$

where $\boldsymbol{C}$ is the equivalent channel matrix.

In sequence, the received signal is transformed into the frequency domain via DFT ($\boldsymbol{F}_N$).

The received frequency domain signal after DFT is:

$$\boldsymbol{S}_r[k] = \boldsymbol{F}_N \boldsymbol{C} \boldsymbol{X}[n] + \boldsymbol{F}_N \boldsymbol{R}_{CP} \boldsymbol{V}[k]. \quad (10)$$

Form Equation (5) we have:

$$\boldsymbol{S}_r[k] = \boldsymbol{F}_N \boldsymbol{C} \boldsymbol{F}_N^{-1} \boldsymbol{S}_d[k] + \boldsymbol{F}_N \boldsymbol{R}_{CP} \boldsymbol{V}[k] \quad (11)$$

$$= \boldsymbol{\Lambda} \boldsymbol{S}_d[k] + \boldsymbol{F}_N \boldsymbol{R}_{CP} \boldsymbol{V}[k]. \quad (12)$$

Knowing that the equivalent channel matrix $\boldsymbol{C}$ is circulant, therefore normal, and any normal matrix can be diagonalized by a pair of unitary matrices, applying DFT and IDFT as unitary matrices, we can notice that $\boldsymbol{\Lambda} = \boldsymbol{F}_N \boldsymbol{C} \boldsymbol{F}_N^{-1}$ is an $N \times N$ diagonal matrix whose elements are the channel frequency response.

After demapping, a frequency equalization is performed. The association of insertion and removal of cyclic prefix with DFT and IDFT transforms makes the equalization very simple. This operation in frequency domain can be accomplished by a pointwise multiplication of the DFT frequency samples characterized by a diagonal matrix. For equalization, minimum mean square error (MMSE) was employed. The equalized signal can be shown to be:

$$\boldsymbol{S}_w[k] = \boldsymbol{W} \boldsymbol{S}_r[k], \quad (13)$$

where $\boldsymbol{W} \in \mathbb{C}^{N \times N}$ is the frequency domain equalizer matrix. After equalization, symbols can be estimated.

B. Power Efficiency

The peak-to-average power ratio (PAPR) is a performance measurement that indicates the power efficiency of the transmitter in communication systems [12]. In general, the PAPR of the $s[n]$ sequence is defined as the ratio between its maximum instantaneous power and its average power [13], [14] that is:

$$PAPR(\boldsymbol{s}[n]) = \frac{max\left(|\boldsymbol{s}[n]|^2\right)}{\frac{1}{p}\sum_{p=0}^{p-1} |\boldsymbol{s}[n]|^2}. \quad (14)$$

As in wireless transmissions in the air, PAPR is an important issue in mobile terminals used in underwater communications.

One of the most serious problems of high PAPR of the transmitted signal is that large peaks may cause serious degradation in system performance when the signal passes through a nonlinear amplifier. It means that an amplifier must have a large linear operating range, which is quite expensive. The nonlinearity cause in-band distortion which might increase bit error rate (BER) and out-of-band radiation.

OFDM systems can provide a type of signal that has the property of having a large variation on the amplitude of transmitted symbols, which means high PAPR.

In addition to this characteristic OFDM has other vulnerabilities: high sensitivity to frequency offset and vulnerability to spectral nulls in the channel. Due to these characteristics, single carrier system (SC-FDM) was analyzed. This analysis is based on the fact that SC-FDM shows better PAPR characteristics, robustness to spectral nulls and lower sensitivity to carrier frequency offset than OFDM [12], [14].

Figure 3 shows the Complementary Cumulative Distribution Function (CCDF) of PAPR for both cases OFDM and SC-FDM. This function represents the probability that the PAPR takes values larger than certain threshold $PAPR_0$ ($Pr(PAPR>PAPR_0)$). We can note that SC-FDM have indeed lower PAPR than OFDM.

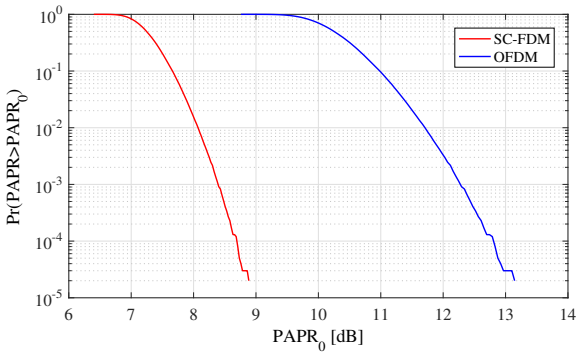

Fig. 3. Comparision of complementary cumulative distribuition function (CCDF) of PAPR for SC-FDM and OFDM for systems with total number of subcarriers N=32, number of input symbols M=32 and digital modulation 4QAM.

Usually, communication systems employ some type of coding to achieve low bit error. In this case the transmitted data bits are encoded at the transmitter and decoded at the receiver to overcome errors. In order to evaluate BER degradation of the transmitted signal caused by its interaction with the channel this work did not utilize any type of encoder.

C. SC-FDM

SC-FDM has a lot in common with OFDM. One difference is a DFT performed on the signal by the transmitter before the subcarrier mapping.

Data symbols are not directly assigned to each subcarrier. After the digital modulation the transmitter performs an M-point DFT to produce a frequency domain representation of the input symbols, $\boldsymbol{S}[k] = \boldsymbol{F}_M \boldsymbol{S}[n]$, $\boldsymbol{F}_M$ is an $M \times M$ DFT matrix. The signal assigned to each subcarrier is actually a linear combination of all modulated data symbols transmitted in the same block.

This system divides the bandwidth into multiple sub-carriers maintaining orthogonality among them, and then maps each of the M-DFT outputs to one of the N orthogonal sub-carriers where ($N \geq M$) [12], [15]. This process is performed by the allocation matrix $\boldsymbol{D}$, defined in (4). As in OFDM, an N-point inverse DFT transforms the subcarrier amplitudes to a complex time domain signal and before transmission a cyclic prefix is inserted at the beginning of each block.

At the receiver, after removing CP, the signal is transformed into the frequency domain via DFT and the mapping on the subcarriers is undone. Still in the frequency domain, such as in OFDM, an MMSE equalizer was applied. Thus, the equalized symbols are transformed back into time domain via inverse DFT and detection takes place in the time domain.

V. Simulation Results

In this section we present experimental results obtained in computational simulations. The experiments carried out consisted of averaging the outcome of 100 transmission blocks, through a channel with bandwidth of 5 kHz (5 kHz–10 kHz) for each system tested. Two Doppler scenarios were tested, $v_t - v_r = 3$ m/s and 5 m/s. We assumed that all paths had the same Doppler scaling factor and the signal-to-noise ratio varied from 0 dB to 20 dB. All three systems had the same spectral efficiency, as follows. For the OFDM $N = 32$ subcarriers were employed, and for SC-FDM $N = 64$ but just 32 were used. The digital modulation employed, 4QAM, provides 2 bits for each complex symbol resulting in 64 bits for each block. The FSK symbol has duration of $T_{block}/16$ and carriers 4 bits of information. Therefore there are 64 bits of information for T_{block} seconds to all transmitted. All transmitted symbol blocks had the same duration T_{block}.

The simulated channel impulse response was given by an FIR approximation with $L_c = 15$ coefficients with gain A_p and additive white Gaussian noise (AWGN) as the model described in Section II. We assumed that the transmission of the message was performed during the channel coherence time, thus we can assume τ_p constant during transmission.

An example of a simulated channel impulse response without Doppler effect is shown in Figure 4.

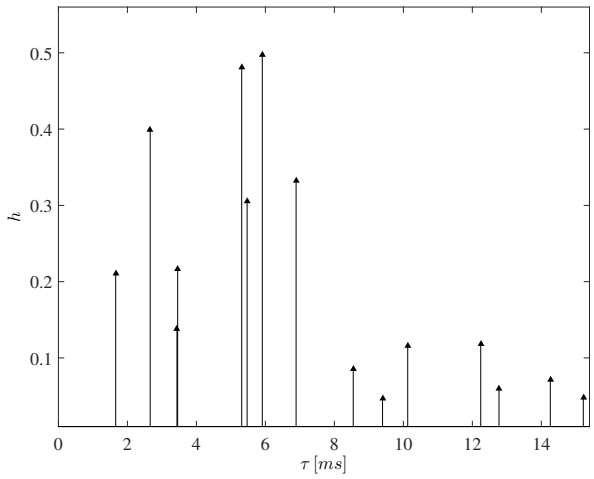

Fig. 4. Impulse response of a time invariant underwater acoustic channel.

The first scenario tested was a transmission in a channel with 15 paths in presence of AWG noise. The results of our simulations are presented in Figure 5, where performance can be evaluated in terms of bit-error rate (BER) as a function of signal-to-noise ratio (SNR) for all modulation schemes. All the results presented are averaged values over 1000 independent runs. The graph shows a better performance of SC-FDM and FSK then OFDM except when we have high SNR. It is still possible to note a similar behavior between SC-FDM and FSK for low SNR.

A second experiment evaluated the performance of the three schemes for a channel with Doppler and multi-path. The behavior of all modulation schemes discussed were evaluated

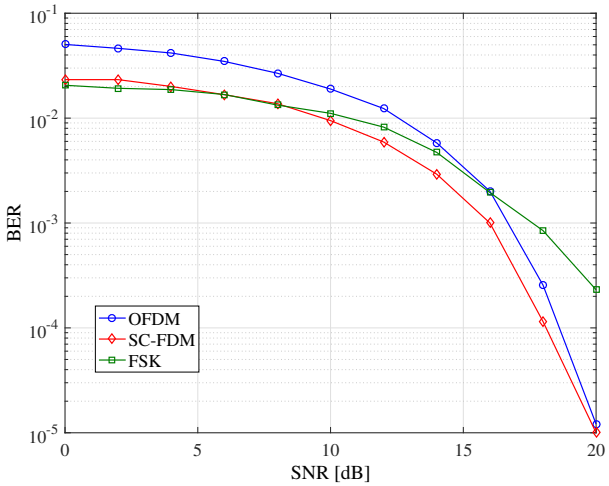

Fig. 5. Performance of FSK SC-FDM and OFDM systems operating in a multipath channel.

in terms of BER as a function of SNR. Figure 6 depicts the obtained results for SC-FDM and OFDM, and Figure 7 for FSK.

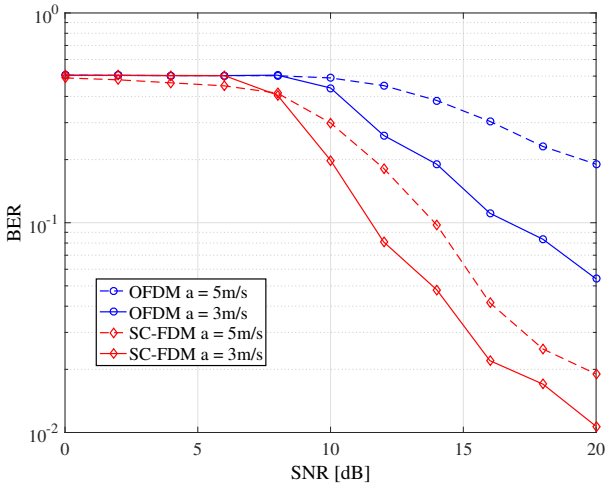

Fig. 6. Comparison among performances of SC-FDM and OFDM systems with MMSE equalizer in a multipath channel with Doppler effect.

In order to evaluate the behavior of these systems in presence of Doppler effect, all these simulations do not employ any type of estimation or Doppler correction.

We can note a severe degradation in performance of the systems when increasing the Doppler scaling factor. The degradation is more pronounced when OFDM and SC-FDM are employed than FSK. For example, FSK can achieve lower value of BER than SC-FDM and OFDM for the same SNR. For SNR equal to 20 dB in FSK we can achieve bit error rate 10^{-3}, whereas in SC-FDM and OFDM just about 10^{-2}. This observation is directly related to the fact that these systems might provide shorter spacing between subcarriers and shorter symbol duration than FSK.

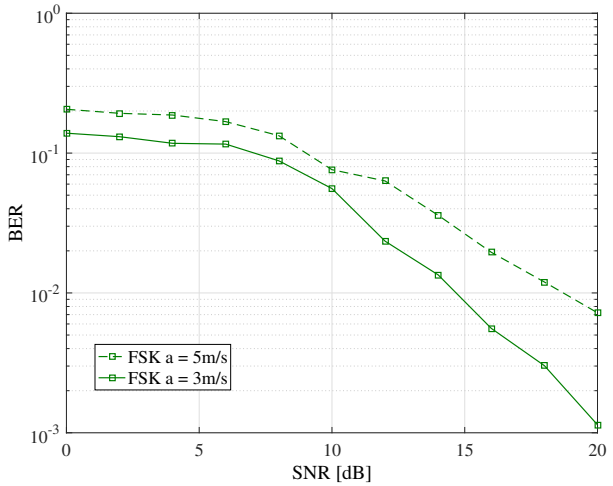

Fig. 7. Comparison among performances of FSK systems with MMSE equalizer in a multipath channel with different Doppler scaling factors.

VI. Conclusions

This paper presents a simulation comparison among three different communication schemes tested in an underwater acoustic scenario with and without Doppler effect. Orthogonal frequency division multiplexing (OFDM) and single-carrier frequency division multiplexing (SC-FDM) were compared to a more simple system, frequency-shift keying (FSK) without any Doppler correction.

From the obtained simulation results, we noticed that the channel effects disrupt the orthogonality among the sub-carriers in SC-FDM and OFDM systems and degrade the BER. In both cases, for a relative velocity $v_t - v_r = 3$ m/s and 5 m/s, we need to introduce some Doppler effect correction technique to avoid performance degradation.

FSK system is less sensitive to Doppler effect than the others tested systems, however its effects also can degrade BER performance.

If low data rate is satisfactory for the application to which the transmission is intended, we can employ FSK as a simple solution for transmission.

We also conclude that FSK systems are more efficient in the presence of Doppler if their carrier separation is greater than in SC-FDM and OFDM systems which means low data rate. But if high data rates are needed for underwater communications, SC-FDM suggests potential advantages as long as transceiver design incorporates modern signal processing techniques to mitigate the harmful effects the communication channel has on the integrity of the signal.

References

[1] T. H. Eggen, A. B. Baggeroer, and J. C. Preisig, "Communication over Doppler spread channels. part I: Channel and receiver presentation," *IEEE Journal of Oceanic Engineering*, vol. 25, no. 1, pp. 62–71, 2000.

[2] P.-J. Bouvet and A. Loussert, "An analysis of MIMO-OFDM for shallow water acoustic communications," in *OCEANS'11*, pp. 1–5, IEEE, 2011.

[3] P.-J. Bouvet, Y. Auffret, A. Loussert, P. Tessot, G. Janvresse, and R. Bourdon, "MIMO underwater acoustic channel characterization based on a remotely operated experimental platform," in *OCEANS'14-TAIPEI*, pp. 1–6, IEEE, 2014.

[4] B.-C. Kim and I.-T. Lu, "Parameter study of OFDM underwater communications system," in *Oceans'00 MTS/IEEE Conference and Exhibition*, vol. 2, pp. 1251–1255, IEEE, 2000.

[5] A. E. Abdelkareem, B. S. Sharif, C. C. Tsimenidis, J. A. Neasham, and O. R. Hinton, "Low-complexity Doppler compensation for OFDM-based underwater acoustic communication systems," in *Proc. OCEANS'11 IEEE-Spain*, pp. 1–6, IEEE, 2011.

[6] S. Zhou and Z. Wang, *OFDM for Underwater Acoustic Communicationn*. UK: Wiley and Sons, 1 ed., 2014.

[7] A. Y. Kibangou, L. Ros, and C. Siclet, "Doppler estimation and data detection for underwater acoustic ZF-OFDM receiver," in *Proc. Wireless Communication Systems (ISWCS'10) 7th International Symposium on*, pp. 591–595, IEEE, 2010.

[8] J. Trubuil and T. Chonavel, "Accurate Doppler estimation for underwater acoustic communications," in *OCEANS'12-Yeosu*, pp. 1–5, IEEE, 2012.

[9] B. Li, S. Zhou, M. Stojanovic, L. Freitag, and P. Willett, "Multicarrier communication over underwater acoustic channels with nonuniform Doppler shifts," *IEEE Journal of Oceanic Engineering*, vol. 33, no. 2, pp. 198–209, 2008.

[10] A. Patel, R. Gupta, and M. Shukla, "Paper performance analysis of OFDM-IDMA and SC-FDMA-IDMA scheme in underwater communication," *Global Journal of Enterprise Information System*, vol. 7, no. 2, pp. 11–17, 2015.

[11] S. Kaddouri, P.-P. J. Beaujean, P.-J. Bouvet, and G. Real, "Least square and trended Doppler estimation in fading channel for high-frequency underwater acoustic communications," *IEEE Journal of Oceanic Engineering*, vol. 39, no. 1, pp. 179–188, 2014.

[12] H. G. Myung, "Introduction to single carrier FDMA," in *Proc. Signal Processing Conference, 2007 15th European*, pp. 2144–2148, IEEE, 2007.

[13] M. C. P. Paredes and M. García, "The problem of Peak-to-Average Power Ratio in OFDM systems," *arXiv preprint arXiv:1503.08271*, 2015.

[14] F. S. Al-kamali, M. I. Dessouky, B. M. Sallam, F. Shawki, and F. A. El-Samie, "Regularized MIMO equalization for SC-FDMA systems," *Circuits, Systems, and Signal Processing*, vol. 31, no. 4, pp. 1423–1441, 2012.

[15] B. Hanta, "SC-FDMA and lte uplink physical layer design," in *Seminar LTE: Der Mobilfunk der Zukunft, University of Erlangen-Nuremberg, LMK*, 2009.